

Operational wave forecasting and two-way interaction of wind and waves

Peter Janssen and Jean Bidlot

European Centre for Medium-Range Weather Forecasts

`< peter . janssen @ ecmwf . int >`

INTRODUCTION

In the context of the **energy balance equation**, we describe some recent progress in our understanding of the interaction of wind and ocean waves. Starting point is the quasi-linear theory of wind-wave interaction as introduced in WAM cycle 4 in 1991. This approach is still used in a number of forecasting systems and we show that up to a wind speed of 25 m/s it gives good results regarding the drag of airflow over the ocean.

Here, we would like to extend the wind-wave interaction approach to the case of strong hurricane winds. Three new aspects are introduced:

- Determine the background roughness length from the stress exerted by the gravity-capillary waves on the airflow
- Solve the stress balance equation in the vertical which results in a nonlinear wind input source function. Nonlinearity is found to be important for wind speeds larger than 20-25 m/s.
- Extend theory to two dimensional propagation.

The programme of this talk is as follows:

I will firstly briefly present the quasilinear theory of wind-wave interaction introduced in 1991 and discuss its quality. This approach produces too much drag for winds above 25 m/s. One of the reasons of the large drag is the assumption of a constant background Charnock parameter. In the new version of the wind-wave coupling this is replaced by a determination of the background roughness from the unresolved **gravity-capillary waves**. Another reason is that for large winds the waves become so steep that **nonlinear** effects on the growthrate of the waves by wind become important and reduce the drag.

Consequences of these extensions of the theory are discussed and in contrast to the 1991 version of the theory for winds above 25 m/s the drag coefficient now decreases with wind rather than showing an increase. This is a reflection of **flow separation**.

Details of the calculations and discussion, in particular regarding the extension to two dimensions, may be found in ECMWF Tech Memo 882 and in our JPO paper “Wind-wave interaction for strong winds”.

If time permits a brief discussion of effects of surface gravity waves on **heat and moisture flux** is given at the end of the talk.

THE 1991 VERSION OF WIND-WAVE INTERACTION

In the main part of this talk I would like to discuss the role of ocean waves in the momentum transfer in the context of a coupled atmosphere-ocean wave model.

Starting from critical layer theory I will present results on the sea state dependence of the momentum transfer and how well the resulting drag compares with observations.

Quasilinear Theory of momentum flux :

According to critical layer theory waves with phase speed c grow when the curvature in the wind profile $U_0(z)$ at the critical height is negative. Introducing the Doppler-shifted velocity $W = U_0(z) - c$, where the critical height z_c follows from the condition $W = 0$, one finds

$$\left. \frac{\partial}{\partial t} F(k) \right|_{wind} = \gamma F(k), \quad \gamma = -\varepsilon \pi c |\chi_c|^2 \frac{W_c''}{|W_c'|},$$

where the wave-induced vertical velocity χ satisfies the Rayleigh equation

$$W \nabla^2 \chi - W'' \chi = 0, \quad \chi(0) = 1, \quad \chi(\infty) = 0.$$

Wave growth results in a slowing down of the airflow according to

$$\frac{\partial}{\partial t} U_0 = (v_a + D_W) \frac{\partial^2}{\partial z^2} U_0 + \frac{1}{\rho_a} \frac{\partial}{\partial z} \tau_{turb}, \quad D_W = \frac{\pi \omega^2 |\chi|^2}{|c - v_g|} F(k),$$

where the turbulent stress is modelled by means of a mixing length model, i.e.

$$\tau_{turb} = \rho_a l^2 \left| \frac{\partial}{\partial z} U_0 \right| \frac{\partial}{\partial z} U_0, \quad l(z) = \kappa(z + z_b),$$

while κ the von Kármán constant and z_b a background roughness length.

For given spectrum $F(k)$ one may search for steady state solutions of the airflow over wind waves by means of an iteration method. The rate of convergence of this procedure was judged by calculating the total stress $\tau_{tot} = \rho_a u_*^2$

$$\tau_{tot} = \tau_v + \tau_{turb} + \tau_w,$$

where $\tau_v = \rho_a \nu_a \partial U_0 / \partial z$ and the wave-induced stress can be shown to be given by

$$\tau_w = - \int_z^\infty dz D_W \frac{\partial^2}{\partial z^2} U_0 = \int d\mathbf{k} \left. \frac{\partial P}{\partial t} \right|_{wind}$$

with wave momentum $P = \rho_w g F(\mathbf{k}) / c$.

The wave spectrum is given by the JONSWAP spectrum with a Phillips parameter α_p which is assumed to depend in a sensitive manner on the wave age c_p / u_* , i.e.

$$\alpha_p = 0.57 (c_p / u_*)^{-3/2},$$

hence young wind waves ($c_p / u_* = 5$) are steep while old wind sea ($c_p / u_* = 25$) is a smooth.

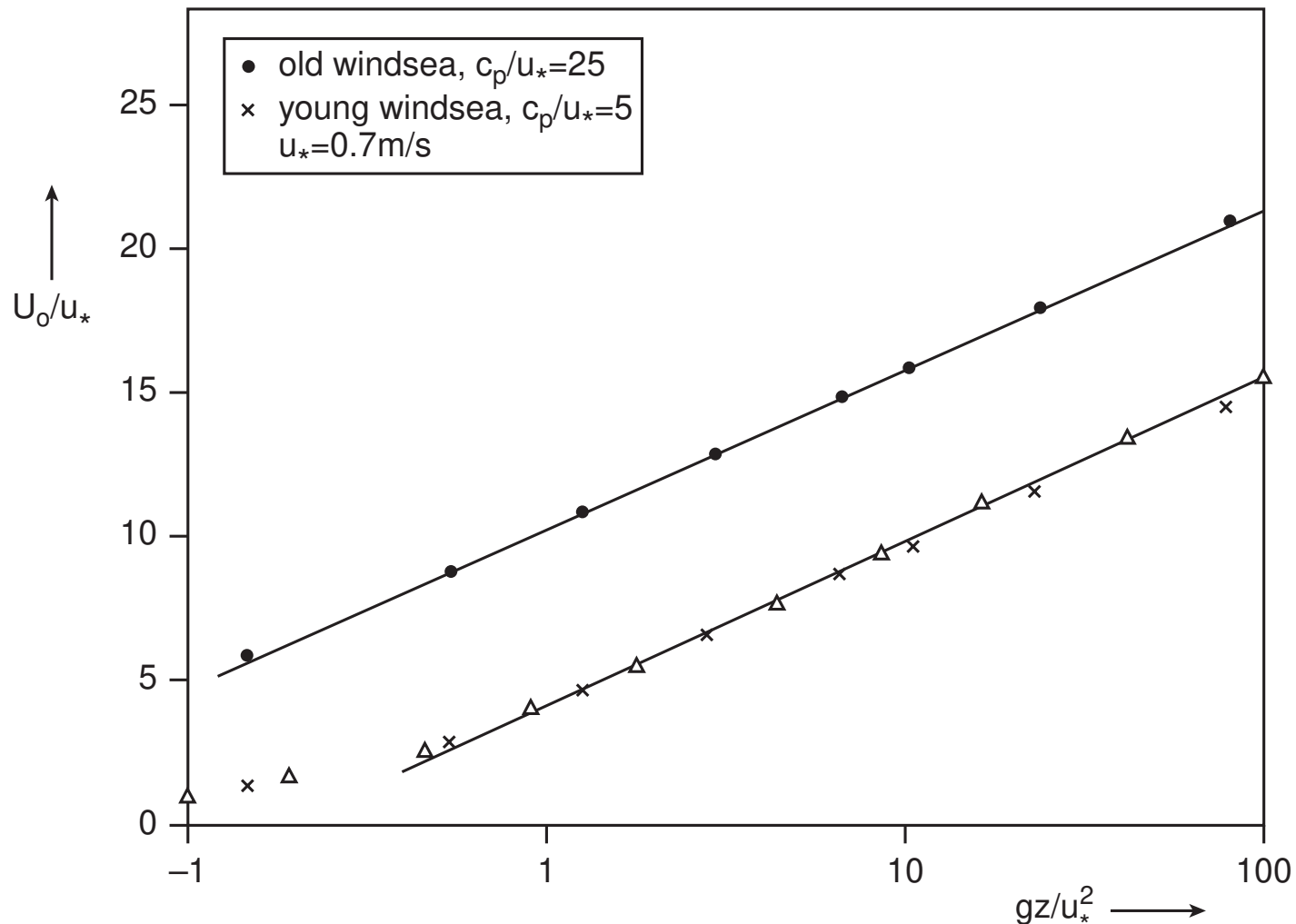


Figure 1: Effect of waves on wind profile for old and young windsea, shown by plotting dimensionless wind speed U_0/u_* as a function of dimensionless height $z_* = gz/u_*^2$. The wind profile parametrization $1/\kappa \log(1 + z_*/z_0^*)$ is denoted by a Δ .

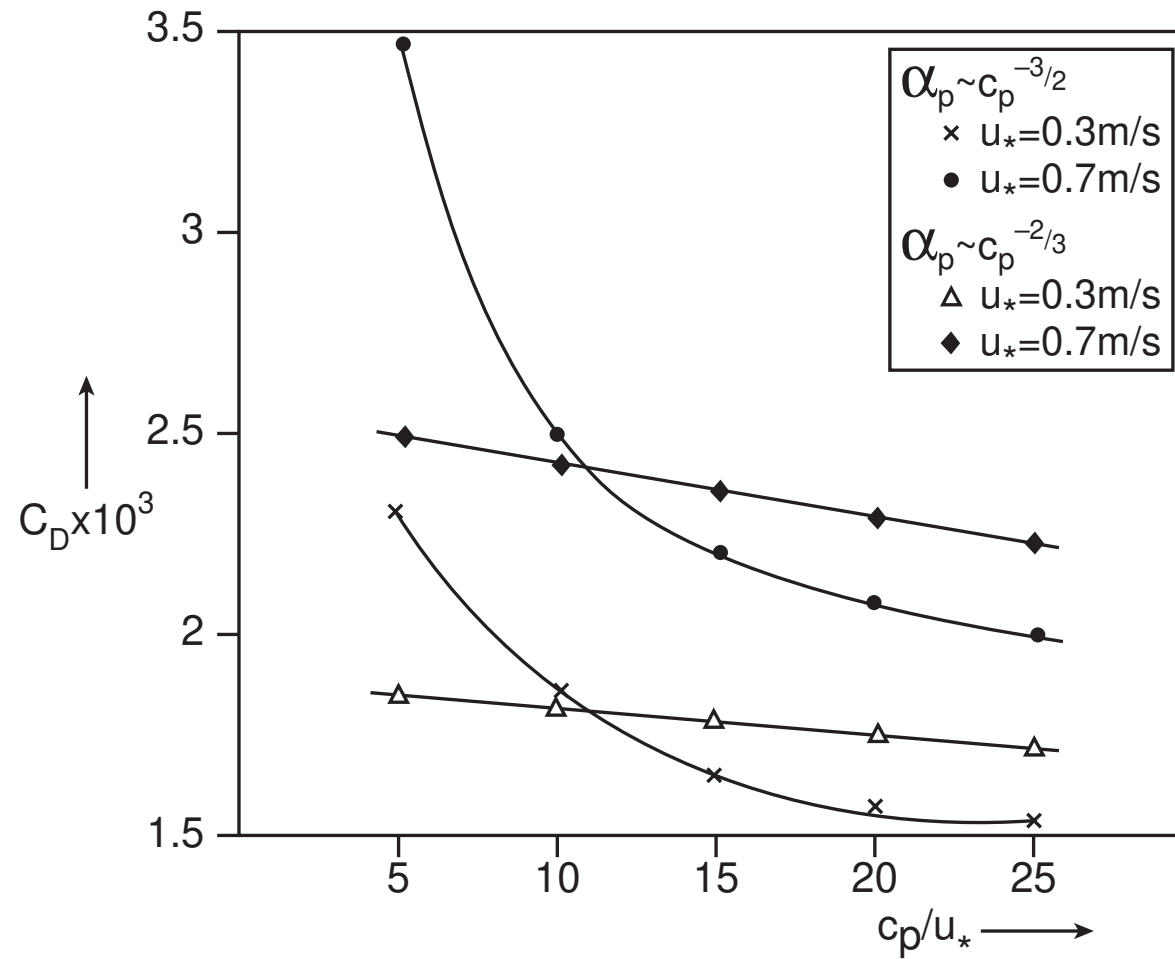


Figure 2: The wave age dependence of the drag coefficient for two different friction velocities.

Parametrization

The numerical results suggest that air viscosity is not important so I start from the stress relation $\tau_{turb} + \tau_w = \tau$, or explicitly, with $l = \kappa(z + z_b)$

$$l^2 \left| \frac{\partial U_0}{\partial z} \right| \frac{\partial U_0}{\partial z} + \tau_w(z) = \tau.$$

In principle one could try to solve this differential equation for wind velocity with boundary condition $U_0(z = 0) = 0$ if one knows the wave-induced stress τ_w . However, things turn out to be simpler if one starts from the following fit of the wind-profile to the numerical data of Janssen(1989)

$$U_0(z) = \frac{u_*}{\kappa} \log \left(1 + \frac{z}{z_0} \right),$$

and determines the τ_w -profile. For $z = 0$ one finds

$$\frac{\tau_w(0)}{\tau} = 1 - \frac{z_b^2}{z_0^2}$$

and therefore the roughness length z_0 becomes

$$z_0 = \frac{z_b}{\sqrt{1 - \tau_w/\tau}} \rightarrow \alpha_{CH} = \frac{gz_0}{u_*^2}.$$

Here, τ_w is obtained from the wave model, while the background roughness length is given by $z_b = \alpha_b u_*^2/g$ with a constant background Charnock parameter $\alpha_b \approx 0.0065$.

Another advantage of using the logarithmic wind profile is that it provides a simple parameterization of the wave growth by wind. In order to obtain the growth rate γ one needs to solve the Rayleigh equation which cannot be solved exactly. Instead, as a starting point a result from Miles (1993) is used who derived an approximate expression for the growth rate obtained by means of asymptotic matching.

Miles (1993) found that

$$\gamma/\omega_0 = \varepsilon\beta \frac{u_*^2}{c^2} \cos^2 \theta, \quad \beta = \frac{\pi}{\kappa^2} y_c \log^4 \left(\frac{y_c}{\lambda} \right), \quad y_c \leq \lambda = \frac{1}{2} e^{-\gamma_E} = 0.281,$$

where $y_c = kz_c$ is a dimensionless critical height and ε is the air-water density ratio.

This expression is valid for slow waves only so in order to also have a reasonable approximation for the long waves parameters were rescaled by replacing $\lambda = 0.281$ by $\lambda = 1$, and by replacing π by the factor 1.2. In addition, in the formula for the critical height, the parameter u_*/c was shifted by a factor $z_\alpha = 0.008$. As a result the following parametrization for the Miles' parameter β is used:

$$\beta = \frac{1.2}{\kappa^2} y_c \log^4 (y_c), \quad y_c \leq 1,$$

where

$$y_c = kz_0 \left(e^{\kappa/x} - 1 \right), \quad x = (u_*/c + z_\alpha) \cos(\theta - \phi), \quad z_\alpha = 0.008.$$

Validation of the approach

- Show that realistic values of drag over the ocean are produced by comparing with eddy correlation data collected for the COARE parameterization of the drag (obtained from J. Edson). In these campaigns winds are below 25 m/s.
- There is also a good agreement of operational results for $C_D(\lambda/2)$ with a parametrization by Huang which was based on observations from 4 major observational campaigns.

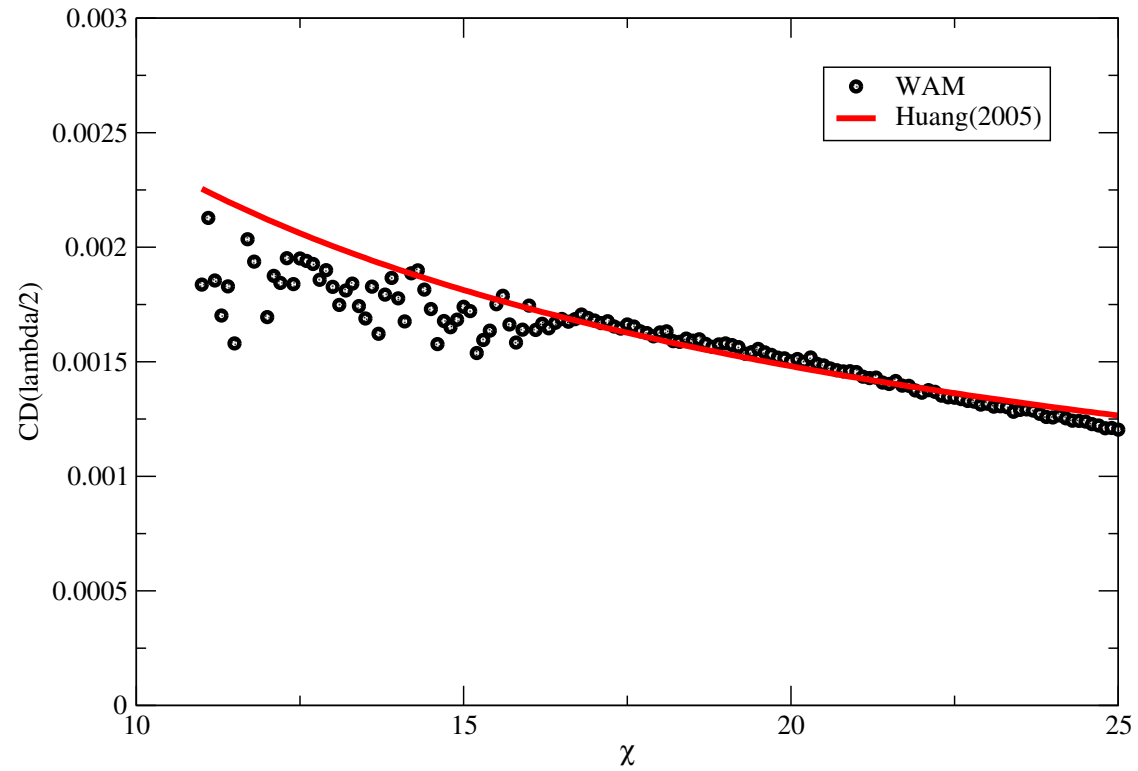


Figure 3: Comparison of ECMWF drag with obs collected by Huang (2005). $C_D(\lambda_p/2) = A\chi^a$, where $\chi = c_p/u_*$ is the wave age, $A = 0.0122$ and $a = -0.704$.

Coupled TCo1279 forecast step3 to step 240 by 3 hrs

start date 2015-03-10, 0 UTC

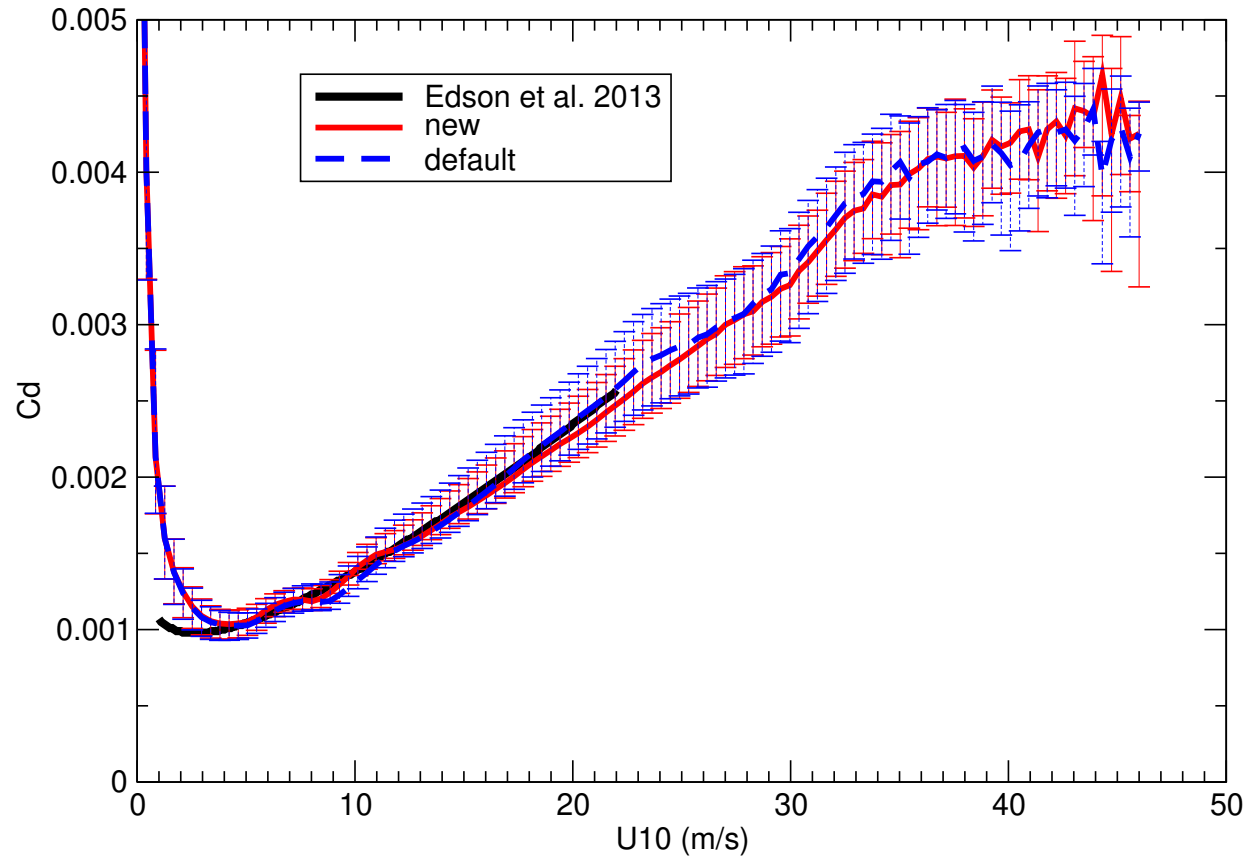


Figure 4: Average Drag Coefficient as function of wind speed according to averaged empirical data from Edson *et al.* and two versions of ecWAM.

Full Nonlinear theory.

The original approach results in drag coefficients that are in good agreement with well-known parametrisations of drag against wind speed or wave age that are obtained from observation campaigns. These observational fits are restricted to wind speeds U_{10} lower than about 25 m/s. Despite this good agreement one may question a number of assumptions underlying the original approach. Here, we discuss the validity of the assumption that the wind profile has a logarithmic shape.

This assumption can be checked by solving the vertical momentum balance equation (in an approximate manner) and one can then calculate the ratio $W_c''/|W_c'|$, which determines the growth rate of the waves by wind. For a logarithmic wind profile this ratio would be equal to $-1/z_c$ but the solution of the momentum balance equation shows that there are small deviations in particular for short waves. The consequence is that the wind input source function depends in a nonlinear way on the wave spectrum.

Denoting by γ_0 the growth rate according to linear theory, nonlinearity is found to renormalise the growthrate γ of the waves by wind in the following manner

$$\gamma = \gamma_0 \frac{1 + N_1}{1 + N_2}$$

where the renormalisation factors N_1 and N_2 depend on the angular average of the product of linear growth rate and the wavenumber spectrum. They read

$$N_1 = \frac{k^3}{\varepsilon \kappa u_*} \int d\theta \gamma_0 F(k, \theta) \sin^2 \theta, \quad N_2 = \frac{k^3}{\varepsilon \kappa u_*} \int d\theta \gamma_0 F(k, \theta).$$

The impact of nonlinearity on the growthrate is shown for two wind speeds in the next graph

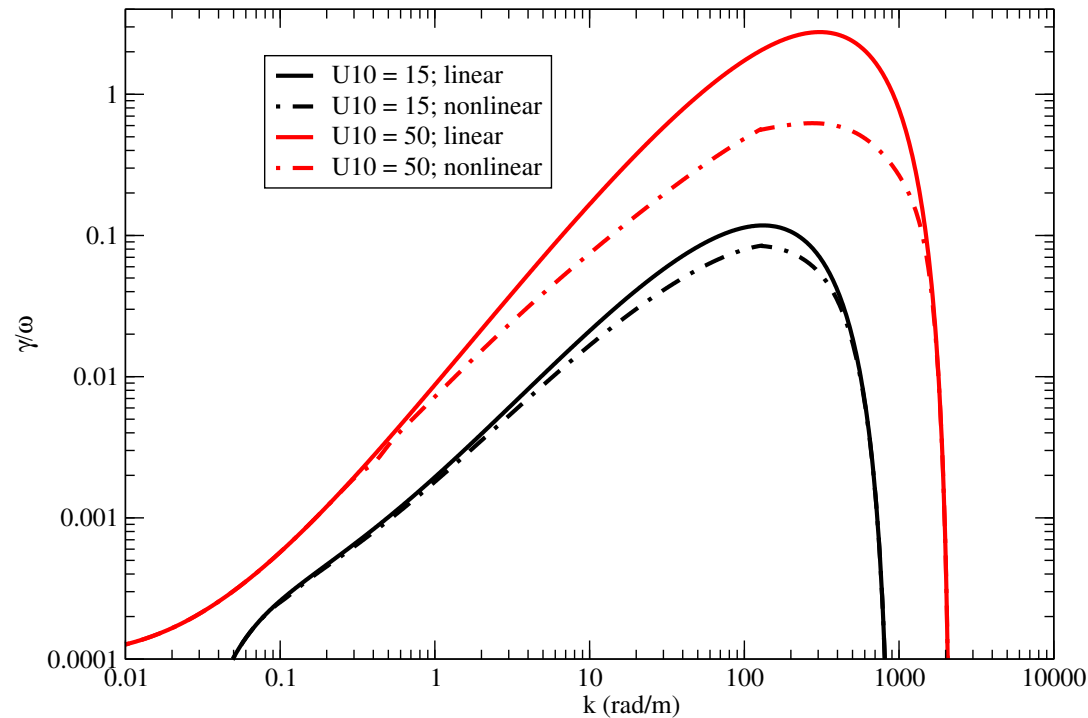


Figure 5: Normalised growthrate as function of wavenumber.

Remark: Note that the growth rate, due to the condition $y_c \leq 1$, both vanishes for very long and very short waves. The growthrate vanishes for a cut-off wavenumber $k_c \approx 1/z_0$ which, for a wind speed of 15 m/s equals to $k_c \approx 800$. This assures a finite wave-induced stress.

WIND-WAVE INTERACTION FOR STRONG WINDS

Extend the theory of **wind-wave generation** to include effects of **gravity-capillary waves** and **nonlinearity**.

A weak point of the present approach is that the background Charnock parameter α_b , which is connected to the gravity-capillary wave stress, is a constant. This cannot be entirely correct because it is known that for large wavenumbers ($k > k_c = 1/z_0$) the momentum transfer from wind to waves is quenched with the result that the wave-induced stress from the shorter waves vanishes. Hence, for given wind speed one should expect that the background Charnock parameter depends on the roughness length and hence on wave age.

A model for the short waves

The model for the short wave spectrum (SCAT, Viers model) is based on the one-dimensional energy balance equation, which is solved under steady state circumstances because the short waves have a very small response timescale. Also, advection of short wave energy is disregarded, and the energy balance equation therefore reads

$$S_{in} + S_{nonl} + S_{visc} + S_{br} = 0,$$

where S_{in} represents the input of wind to waves, S_{nonl} describes three- and four-wave interactions, S_{visc} describes viscous dissipation, and S_{br} describes dissipation due to whitecapping.

The energy balance equation is solved as a boundary value problem in wavenumber space by providing the **energy flux** from the long to the short waves at a boundary $k = k_{3w}$ which is basically the wavenumber where three-wave interactions start to become important.

In order to determine the energy flux at the boundary $k = k_{3w}$, knowledge of the gravity part of the wave spectrum is required. The spectrum $F(k)$ at the boundary is given by

$$F(k_{3w}) = \frac{1}{2} \alpha_p k_{3w}^{-4},$$

so that at the boundary the spectrum is given by the Phillips' spectrum with Phillips parameter α_p which in practice depends on wave age χ and can be obtained from the model spectrum.

According to the JONSWAP observations one finds the scaling relation

$$\alpha_p = A \chi^{-B},$$

with $A = 0.24$ and $B = 1$. The above scaling law suggests that the Phillips parameter would continue to increase for decreasing wave age χ , but since waves do have a limiting steepness it seems likely that also **the Phillips parameter is limited.**

To make sure that this limitation is adhered to in the wave model the Phillips parameter is forced to be below the maximum value $\alpha_{max} = 0.031$. It is remarked that the choice for a limiting steepness and Phillips' parameter will have important consequences for the behaviour of the surface stress and wave height for young wind seas.

For wavenumbers higher than k_{3w} we enter the gravity-capillary range so that three-wave interactions become important. We only discuss a theory for the one-dimensional wavenumber spectrum $F(k)$. Here, the spectrum is related to the Fourier transform of the autocorrelation of the surface elevation η , and is normalized in such a way that $\int_0^\infty kdkF(k) = \langle \eta^2 \rangle$, where $\langle \eta^2 \rangle$ is the wave variance. The wave energy E then follows from

$$E = \rho_w \frac{\omega^2}{k} F(k).$$

Here we shall only consider **pure** gravity-capillary waves with dispersion relation $\omega(k) = \sqrt{gk + Tk^3}$, where g is acceleration of gravity and T is surface tension.

Wind Input

For the input source function we take

$$S_{in} = \gamma_{in} F,$$

where γ_{in} is given by the one-dimensional version of the nonlinear wave growthrate. After some rearrangement one finds

$$\gamma_{in} = \gamma_0 \frac{1 + \alpha_1 \gamma_0}{1 + \alpha_2 \gamma_0}$$

with

$$\alpha_1 = \alpha_2/6 \text{ and } \alpha_2 = \Delta_\gamma \frac{k^3 F(k)}{\kappa \varepsilon u_*}$$

while Δ_γ is a directional factor determined in an empirical manner. Furthermore, $\gamma_0 = \varepsilon \beta \omega u_*^2 / c^2$ and β is given as before.

Nonlinear transfer

Following Kitaigorodskii (1983), it is assumed that the nonlinear transfer is a local process in wavenumber space, and introducing the energy flux $\Phi(k)$ one thus has

$$S_{nonl} = -\frac{1}{k} \frac{\partial}{\partial k} \Phi(k)$$

Only three wave interactions will be considered in this talk. On dimensional grounds the expression for $\Phi(k)$ then reads

$$\Phi(k) = \alpha_3 \frac{c^4}{v_g} B^2$$

where v_g is the group velocity $\partial\omega/\partial k$, B is the angular average of **the degree of saturation** (Phillips, 1985),

$$B = k^4 F(k)$$

while α_3 gives the strength of the three-wave interactions. Note that α_3 should vanish in the gravity wave regime because three-wave interactions are not possible in the gravity domain. For this reason k_{3w} is chosen in such a way that it is connected to the

minimum in the phase velocity $c = \omega/k$. This minimum occurs at $k = k_0 = \sqrt{g/T}$ and therefore

$$k_{3w} = y \sqrt{\frac{g}{T}},$$

where the parameter y is typically less than one. A satisfactory choice that was tried is $y = 1/2$, but more refined choices have been proposed as well by J. Janssen and H. Wallbrink (1997).

Exact solution of short-wave energy balance.

Combining now the explicit expressions for the source terms, the energy balance equation becomes

$$\frac{\partial}{\partial k} \Phi(k) = \Gamma \frac{\omega^2}{k^4} B$$

where the parameter Γ is defined as

$$\Gamma = \gamma_{in} - \gamma_d$$

and hence gives the net effect of wind input and dissipation by breaking and viscosity. This energy balance equation may be solved exactly with the following result for the degree of saturation

$$B = \left(\frac{v_g}{\alpha_3} \right)^{1/2} c^{-2} \left\{ \Phi_0^{1/2} + \frac{1}{2\alpha_3^{1/2}} \int_{k_{3w}}^k dk \frac{\Gamma}{k^2} v_g^{1/2} \right\}$$

where Φ_0 is the value of the energy flux at $k = k_{3w}$.

The first term of this solution is directly related to the effect of three-wave interactions and is called the inertial sub-range spectrum. Effects of input and dissipation are represented by the second term and result in a usually small modification to the inertial sub-range.

A graph of the combined gravity wave spectrum (i.e. JONSWAP) and the short-wave spectrum is shown for a wind speed of 15 m/s and different wave ages next.

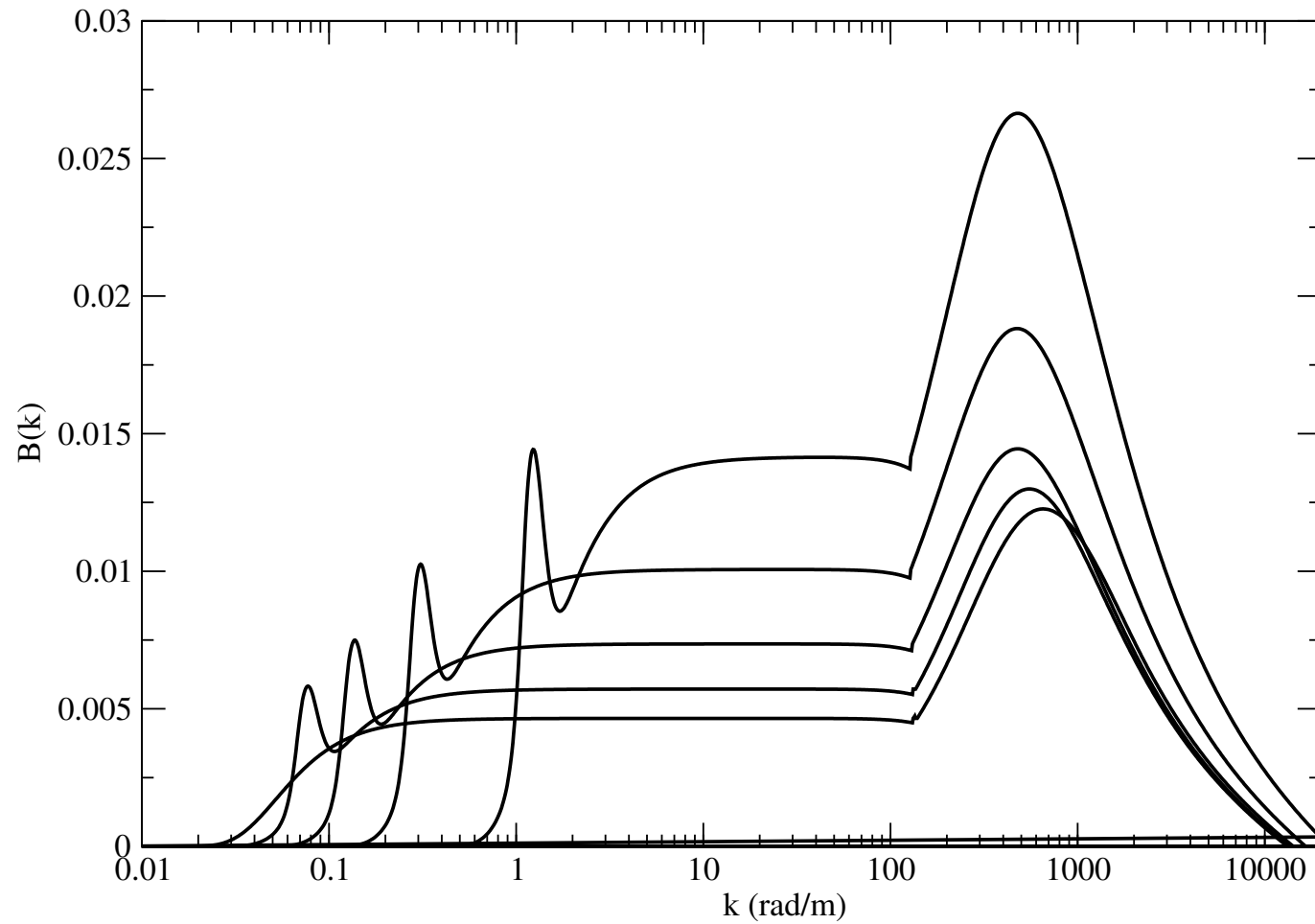


Figure 6: The wave age dependence (between 5 and 25 in steps of 5) of the degree of saturation spectrum as function of wavenumber for a wind speed of 15 m/s.

DETERMINATION OF SURFACE STRESS.**Method**

The present model of the sea state now consists of two parts. The spectrum of the long gravity waves is provided by a wave prediction system while the spectrum of the short waves is given by the short-wave model. Both models assume that the stress τ_a or the friction velocity $u_* = \sqrt{\tau_a/\rho_a}$ is given and at the same time determine the stress. Assuming steady state conditions the surface stress is obtained by finding a solution of the conservation of momentum law at the surface:

$$\tau_a = \tau_v(u_*) + \tau_w(u_*),$$

by means of iteration. In this manner a consistent solution for the spectrum of short and long-waves is obtained and at the same time a consistent estimate of the stress over growing wind waves is found. Here, $\tau_v = \rho_a \bar{v}_a \partial U_0 / \partial z$, with $\bar{v}_a = v_a / 25$, and the wave-induced stress is given by the sum of the low frequency gravity wave stress

and the short wave stress,

$$\tau_w = \tau_{w,lf} + \tau_{w,hf} = \int_0^\infty k dk \int_0^{2\pi} d\theta \gamma P$$

with wave momentum $P = \rho_w \omega(\mathbf{k}) F(\mathbf{k})$, while γ is the renormalized growthrate. As we now have an explicit model for the background roughness (obtained from the short wave stress), the turbulent stress vanishes at the surface. In fact, one finds for the background roughness length

$$z_b = z_0 \sqrt{\frac{\tau_{w,hf}}{\tau_a}}.$$

Climatological results

Using operational results obtained with the coupled IFS-ecWAM model one finds that on average there is a relation between wave age χ and wind speed U_{10} . In the wind speed range of $0 < U_{10} < 25$ it is approximately given by

$$\chi = \frac{35}{1 + 0.005U_{10}^2}$$

and it is assumed that the relation also holds for larger wind speed. The above relation expresses that, in agreement with one's expectations, the stage of development of the sea state generated by low wind speed events is much older than of large wind speed events.

This allows to obtain the average drag coefficient as function of wind speed by assuming that the gravity waves follow the JONSWAP spectrum with a Phillips parameter depending on wave age.

Next show results of drag coefficient over a wind speed range of 80 m/s and also results for the dimensionless background roughness length are shown.

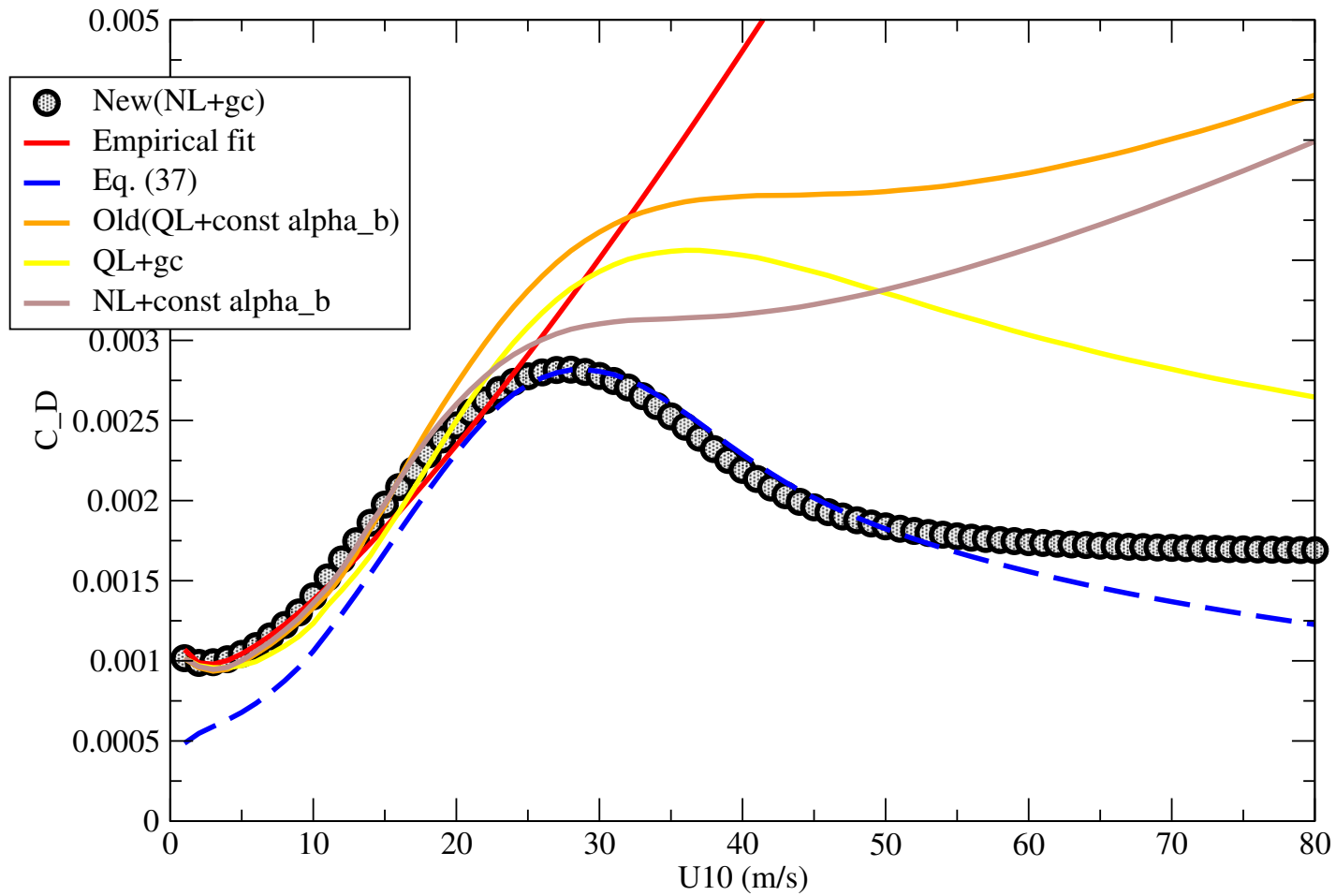


Figure 7: The climatological dependence of the drag coefficient C_D on wind speed U_{10} in the range of 1 to 80 m/s according to the old and the new approach.

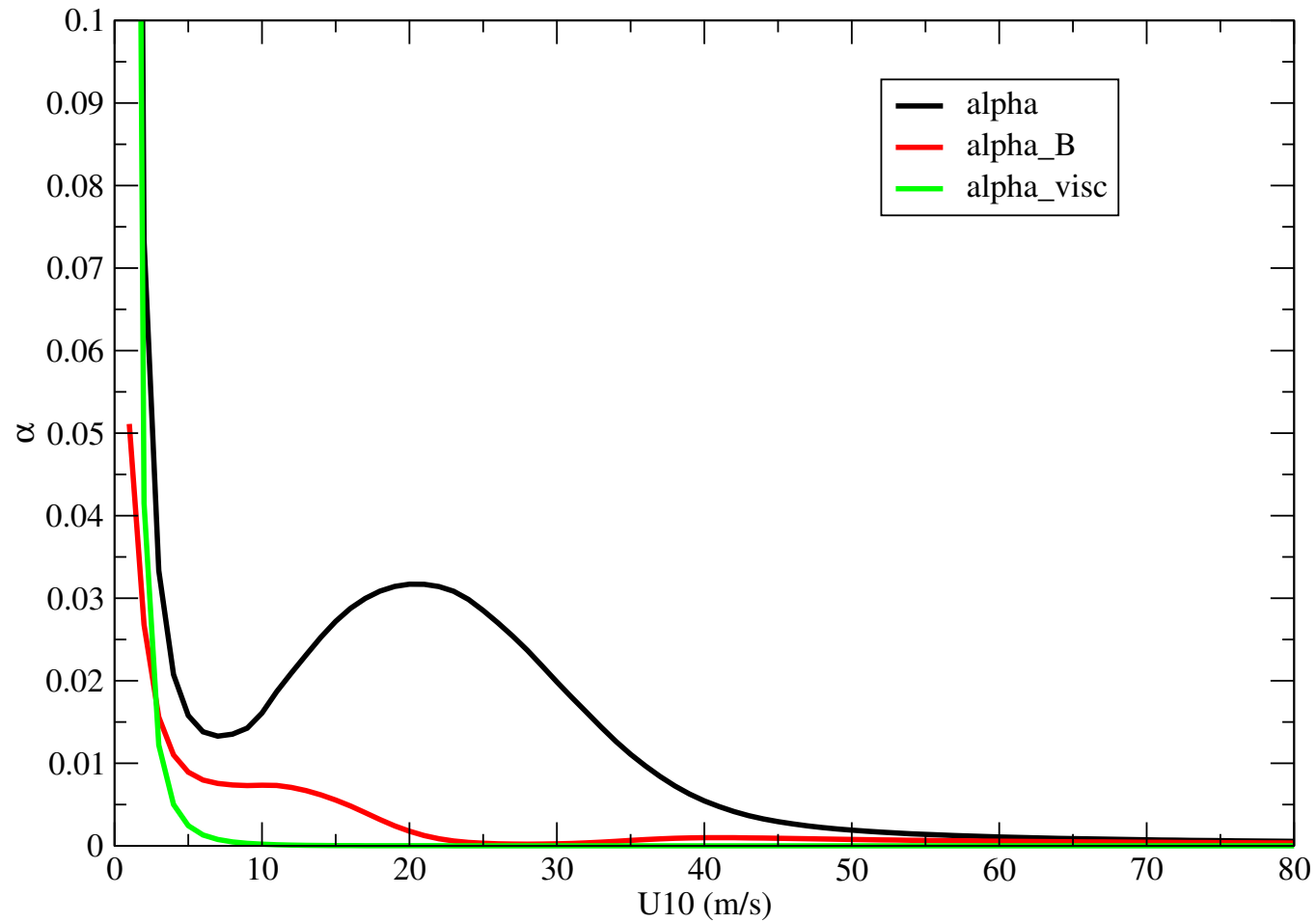


Figure 8: Climatological Charnock parameter α and background Charnock parameter α_b as function of wind speed U_{10} .

Pre-operational Results

We implemented the new approach in a test version of the ecWAM model.

First results regarding drag coefficient and mean square slope look encouraging. For strong winds we see that the nonlinear wind input causes a reduction of C_D with wind speed but the reduction is not as pronounced as in the climatological results. The reason for this is that for large winds the average wave age is larger than assumed in the climatology.

Coupled TCo1279 forecast step 1 to step 72 by 1 hrs

start date 2019-03-22, 0 UTC

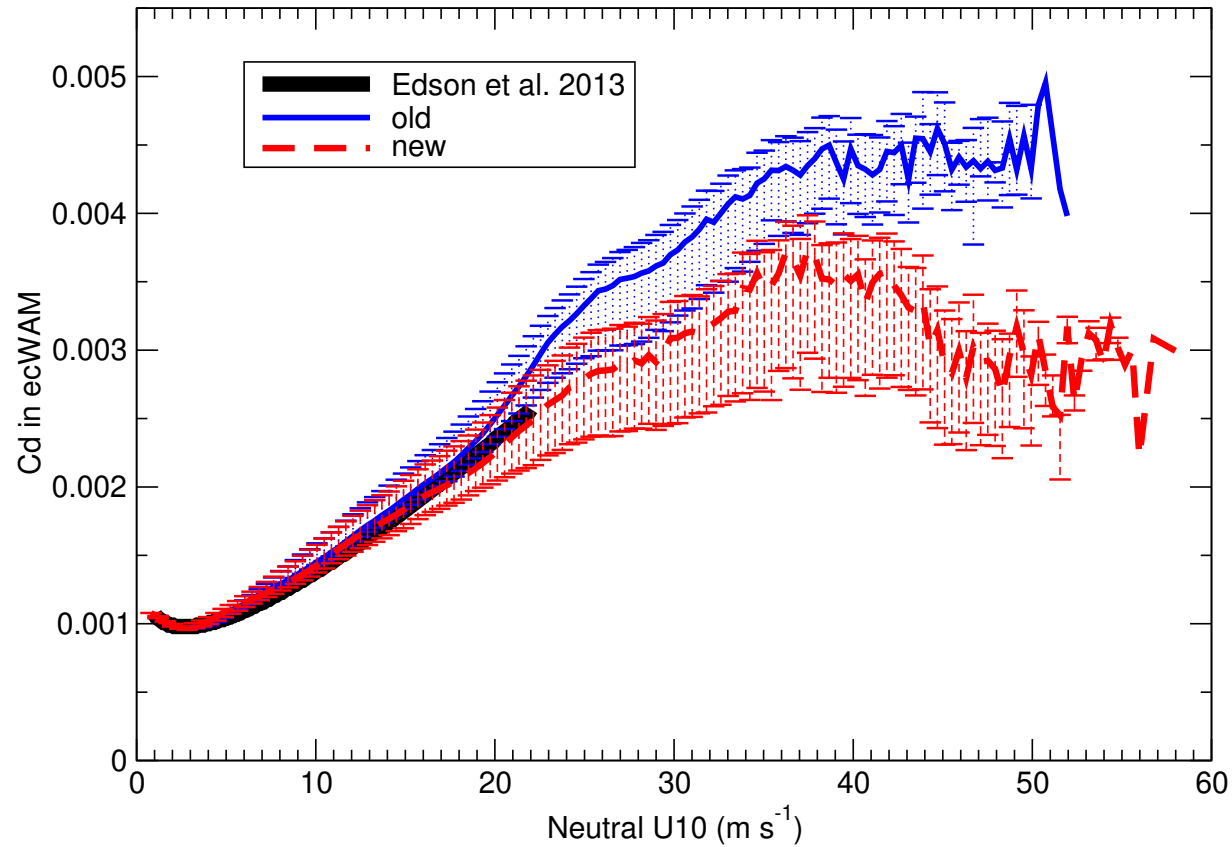


Figure 9: The climatological dependence of the drag coefficient C_D on wind speed U_{10} in the range of 1 to 80 m/s according to the old and the new approach.

Coupled TCo1279 forecast step 1 to step 72 by 1 hrs
start date 2019-03-22, 0 UTC

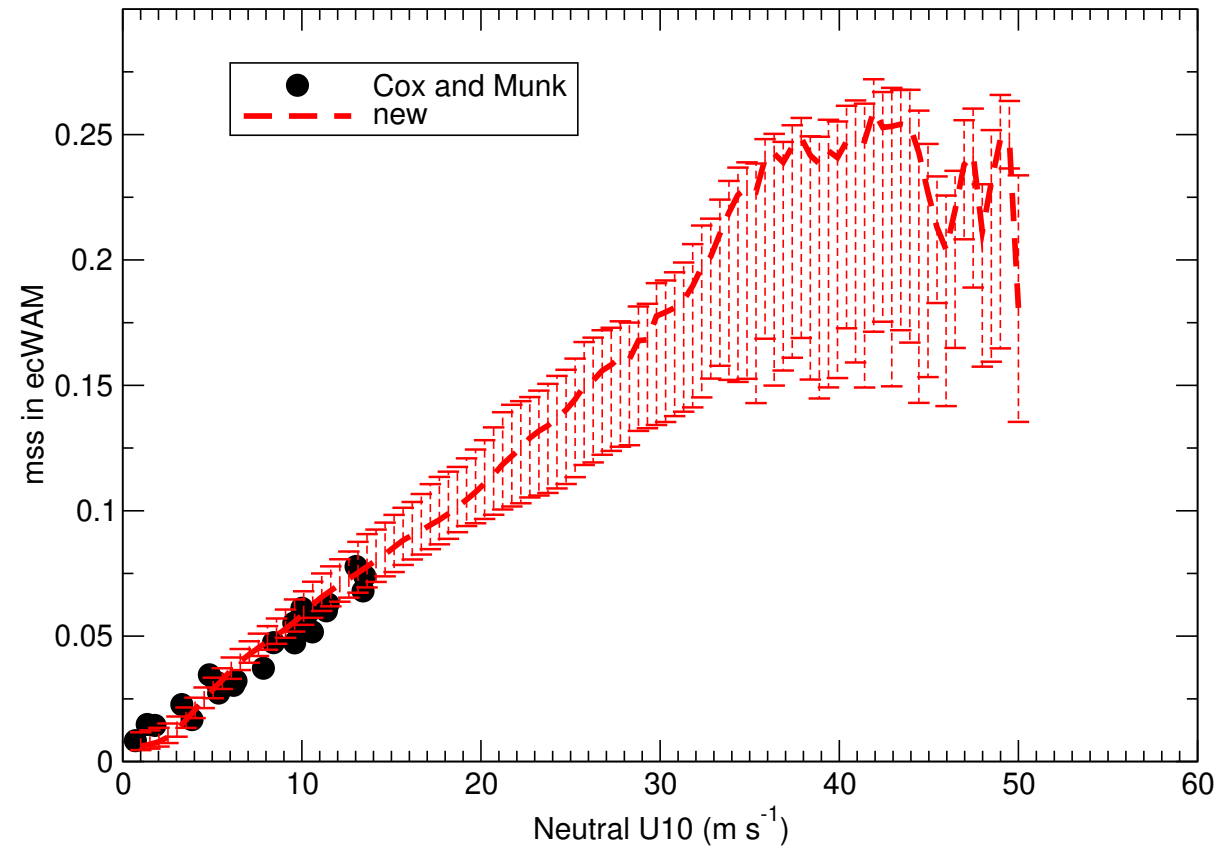


Figure 10: Average mean square slope as function of wind speed U_{10} according to a test version of ecWAM and a comparison with observations from Cox and Munk.

Coupled TCo1279 forecast step 1 to step 72 by 1 hrs

start date 2019-03-22, 0 UTC

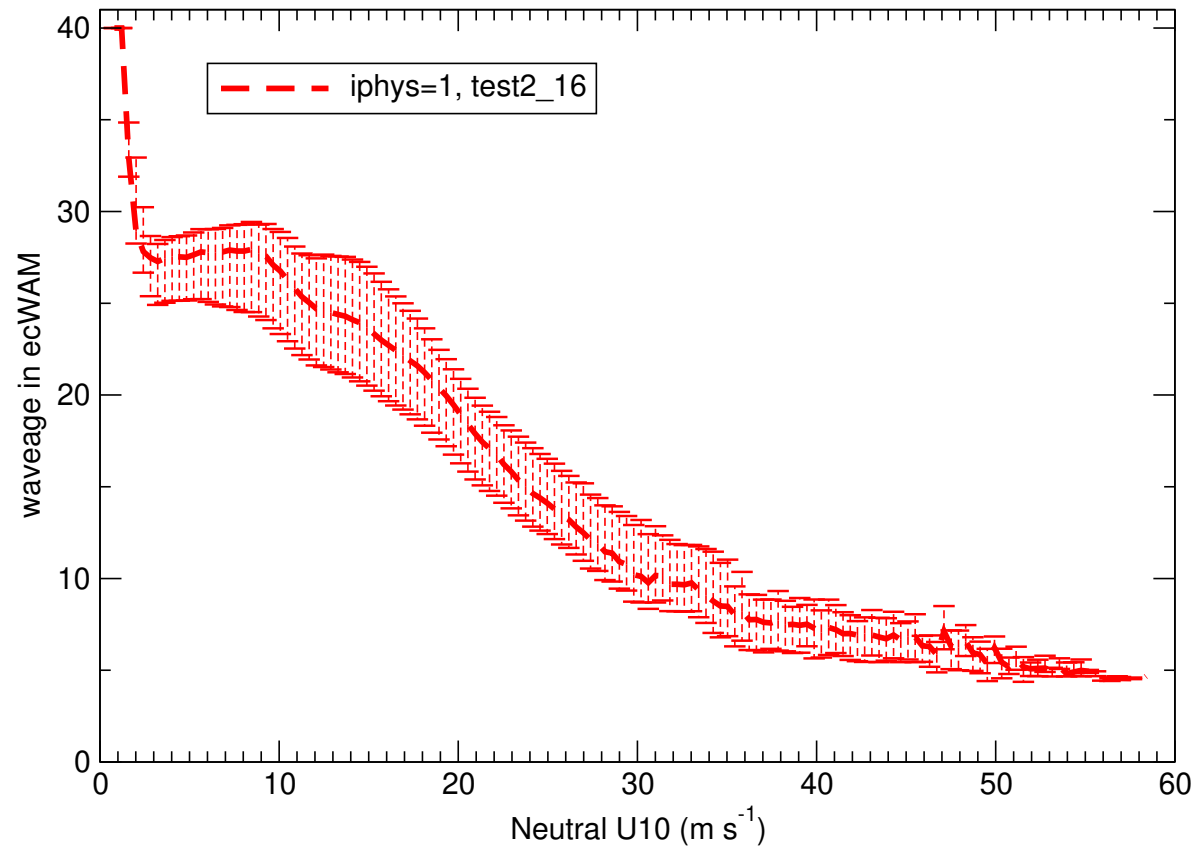


Figure 11: Average wave age of windsea as function of wind speed U_{10} according to a test version of ecWAM.

CONCLUSIONS

- Although we know that there has been considerable progress in operational wave forecasting over the past 25 years that does not mean that we are at the end of the journey.
- There are still a number of important questions to be solved. For example, the wind-wave interaction approach is extremely simple and might require improvements (essentially it is now one-dimensional theory as vorticity is conserved, effects of vortex stretching need to be included). Although I have no details given for this there is now a two-dimensional version of the wind-wave approach, which includes vortex stretching.
- Nevertheless, we are able to give already fairly accurate estimates of the stress (and heatflux) over the oceans for wind speeds, say, less than 25 m/s. We now need reliable estimates for surface stress in hurricane conditions in order to validate models such as the one presented here.

Theory and parametrization of heat flux

Extend the theory of **wind-wave generation** to include thermal **stratification**.

In the passive scalar approximation the evolution of **mean temperature** is found to be

$$\frac{\partial}{\partial t} T_0 = \frac{\partial}{\partial z} \left\{ \left(D_w + l^2 \left| \frac{\partial U_0}{\partial z} \right| + \delta v_z \right) \frac{\partial}{\partial z} T_0 \right\}.$$

where it is assumed that close to the surface the heat transport is determined by molecular conduction, which gives the additional diffusivity δv_z .

Assume steady state and introduce the heat flux q_* . Integrating the T-equation one finds

$$\left\{ D_w + l^2 \left| \frac{\partial U_0}{\partial z} \right| + \delta v_z \right\} \frac{\partial}{\partial z} T_0 = q_*,$$

which is a differential equation for the air-temperature profile subject to the boundary condition that $T_0(z=0) = T_S$ with T_S the sea surface temperature.

Using a parametrization for the wave diffusion coefficient from Janssen (1997),

$$D_w = 2\kappa u_* \frac{(z + z_b)(z_0 - z_b)}{z + z_0},$$

and solving the differential equation for $\Delta T = T_a - T_s$ with boundary condition that $\Delta T = 0$ at $z = 0$, gives a logarithmic profile with 'thermal' roughness z_T ,

$$\Delta T = \frac{q_*}{\kappa u_*} \log \left(\frac{z}{z_T} \right)$$

with $z_T = (z_v(z_0 - z_b))^{1/2}$ and $z_v = \delta v_z / \kappa u_*$.

Note that by definition $\tau = C_D(10)U_{10}^2$ and $q_* = C_q(10)U_{10}\Delta T_{10}$ so that from the wind and temperature profile one now immediately finds expressions for the drag coefficient C_D and the Dalton number C_q :

$$C_D(10) = \left\{ \frac{\kappa}{\log(10/z_0)} \right\}^2$$

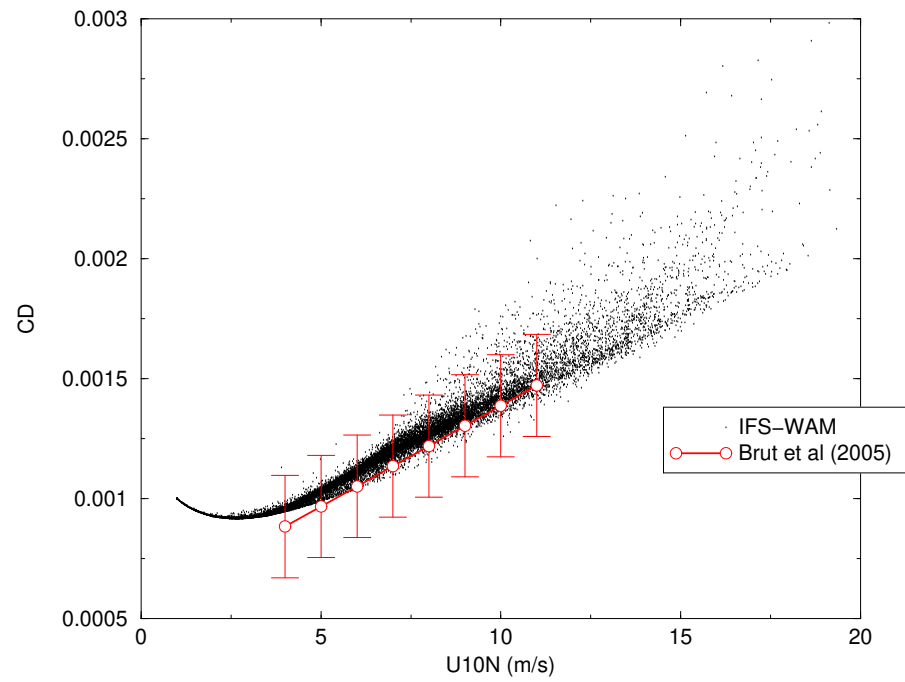
while

$$C_q(10) = \frac{\kappa}{\log(10/z_T)} C_D^{1/2}$$

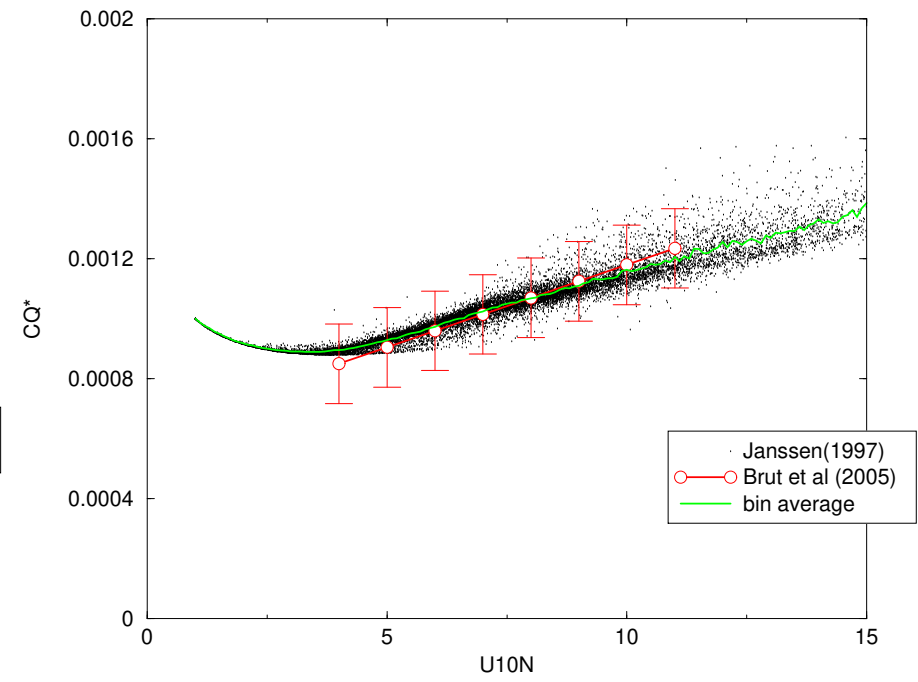
It is straightforward to evaluate these coefficients from ECMWF's IFS. Results show, in agreement with Brut *et al.* (2005), an increase of C_D with wind while C_q also increases with wind but to a lesser extent.

However, result for C_q is in sharp contrast with HEXOS which suggests a constant for the Dalton number. But, subsequent work by Smedman *et al.* (2007) (and also Oost *et al.* (2000)) suggests that C_q increases with wind speed.

CD versus neutral wind



CQ^* versus U_{10N}



Impact on Hurricane Katrina

I have performed a number of sensitivity experiments on hurricane Katrina to test sensitivity to the formulation of the heat and moisture flux. The control experiment is the operational IFS which presently consist of a coupled atmosphere, ocean-wave model. In this model the following representation of the thermal roughness is used

$$z_T = \delta \frac{V}{u_*}, \quad \delta = 0.4, 0.6.$$

When substituted in the expression of the Dalton/Stanton number,

$$C_q = C_D^{1/2} \frac{\kappa}{\log(10/z_T)},$$

this choice of thermal roughness results in a Dalton/Stanton number that is almost independent of wind speed (which agrees with HEXOS).

The next viewgraphs show results of a T 511 simulation with the IFS for surface pressure and significant wave height and the differences between the experiment (with seastate dependent thermal roughness) and control. Impact is quite substantial.

Impact on Tropical Circulation

In the past 5-10 years work has been underway to develop a comprehensive coupled forecasting system (atmosphere, ocean-wave, ocean-circulation, and a sea-ice model). This configuration produces operational deterministic and ensemble forecasts since June 5, 2018.

In the context of this fully coupled system (CY43R1 with resolution TCO 400, corresponding to a spatial resolution of 30 km), I now show impact of the new formulation for the heat flux on the tropical circulation by doing forecasts over a period of one year. The control forecasts were performed with the heatflux formulation that has almost no wind speed dependence. Results of these 10-day forecasts are verified against the operational analysis.

Comparing the verification results for e.g. geopotential height shows a significant reduction in forecast error for the experiment with sea-state dependent thermal roughness.

Earlier experiments with a forecast system with fixed SST (so no dynamic ocean) showed much smaller impact!

Change in error in Z (Sea state heat and moisture fluxes–Reference)

1–Jun–2016 to 31–May–2017 from 356 to 365 samples. Cross-hatching indicates 95% confidence. Verified against 0001.

